



Radiological risk assessment of beaches from volcanic oceanic islands: A case study of the Eastern Canary Islands (Spain)[☆]

Ana del Carmen Arriola-Velásquez, Alicia Tejera^{*}, Héctor Alonso, Neus Miquel-Armengol, Jesús G. Rubiano, Pablo Martel

Department of Physics, Instituto Universitario de Investigación en Estudios Ambientales y Recursos Naturales i-UNAT, Universidad de Las Palmas de Gran Canaria, Campus de Tafira, 35017, Las Palmas de Gran Canaria, Spain

ARTICLE INFO

Keywords:

Radionuclides
Volcanic islands
Coastal sediments
Radiological hazard index

ABSTRACT

This work constitutes the first survey that allows the establishment of baseline levels of environmental radioactivity in beach sands from the volcanic oceanic islands of La Graciosa, Lanzarote, Fuerteventura and Gran Canaria. Activity concentration values of ^{226}Ra , ^{232}Th and ^{40}K were measured by gamma spectroscopy in 108 samples, collected from 39 beaches across the whole study region. The radiological hazard risks associated with these sands were studied. The mean absorbed dose rate in the study region was 20 nGy h^{-1} , which is below the world average value. The mean outdoor annual effective dose for the beaches studied was 0.025 mSv y^{-1} , which is within the internationally accepted safe limit. Additionally, the assessment of the radium equivalent showed that all samples from the Eastern Canary Islands are below the safe limit of 370 Bq kg^{-1} . Despite not posing any radiological risk to the human population, the radiological hazard indices obtained in Gran Canaria were significantly higher than those of other islands. These significant differences seem to be related to the presence of sediments in the beaches of Gran Canaria that have their origin in lithologies with higher activity concentration values of ^{226}Ra , ^{232}Th and ^{40}K that are not present in the rest of the islands.

1. Introduction

Human exposure to ionizing radiation comes from different sources, including medical procedures, nuclear weapon testing, nuclear accidents, natural background radiation and exposure to artificial or natural sources of radiation due to different occupations (UNSCEAR, 2008). However, it is known that, for most individuals, the largest component of their total radiation exposure is due to natural background radiation (UNSCEAR, 2008, 2000). This natural background radiation mainly originates from the primordial radionuclides that constitute the Earth's crust. These primordial radionuclides include ^{40}K and those from the decay series ^{238}U , ^{232}Th and ^{235}U (Froehlich, 2010). The activity concentrations of these radionuclides across different parts of the world depend on the local geology and, thus, baseline studies of these natural background radiation levels are necessary, to be able to identify radiological hazards that can affect the human population.

Coastal and beach areas are very important to the general public, due to their economic and ecological value, and radiological hazard

assessments have been carried out in different coastal areas around the world (Abbasi et al., 2020; Akpan et al., 2020; Al Shaaibi et al., 2023; Alfonso et al., 2014; Awad et al., 2022; Khandaker et al., 2019; Licinio et al., 2021; Rao et al., 2009; Shuaibu et al., 2017). In some of the studies, extremely high doses were reported in India (Vineethkumar et al., 2020), Brazil (Vasconcelos et al., 2011) and Malaysia (Shuaibu et al., 2017). These high doses were associated with the presence of monazite in sand grains, a mineral with high activity concentration values of ^{232}Th (Md. Jaffary et al., 2019). This represents an example of how geological variations in sediments around the globe can affect the population's radiation exposure. Thus, it is important to control the natural background radiation levels in high-value areas for humans, such as beaches.

In the case of the Eastern Canary Islands (La Graciosa, Lanzarote, Fuerteventura and Gran Canaria), studies of environmental radioactivity have focused on the soils of the islands (Arnedo et al., 2017) and groundwater (Alonso et al., 2015). Nevertheless, only a single study on beaches was found in the literature (Arnedo et al., 2013). This is striking,

[☆] This paper has been recommended for acceptance by Jörg Rinklebe.

^{*} Corresponding author.

E-mail address: alicia.tejera@ulpgc.es (A. Tejera).

considering the fact that the Canary Islands represent one of the third most touristic areas in Spain, receiving more than 12 million tourists in 2022 (INE, 2022); the majority of those tourists were drawn to the islands by their beaches, which can be enjoyed all year long. Additionally, the Eastern Canary Islands are located within the main commercial routes between Europe, Africa and America; the port of La Luz in Gran Canaria is the fourth largest port in Spain. This means that many different types of ships (oil product tankers, crude oil tankers, bulk carriers, oil drilling platforms, container ships, ferries and cruise ships) arrive on the islands on a daily basis or pass by en-route to other destinations (MarineTraffic, 2023; Tichavska and Tovar, 2015). Therefore, not only the beaches of the Eastern Canary Islands are places of high occupancy throughout the year, but they also are under the constant threat of suffering some contamination originated in some of the many ships that arrive at its coasts every day. The presence of high concentrations of natural radionuclides in some of these ships, like in the scales that are generated in the pipes of oil drilling (Bou-Rabee et al., 2009), could lead to some radiological hazards that would affect not only the residents on the islands, but also the millions of tourists that visit their beaches every year.

Considering all of this, the main objective of this work is to establish reference levels of environmental background radioactivity on the beaches of the Eastern Canary Islands so any possible radiological contamination that could arrive on the beaches through seawater can be detected. For this purpose, intertidal sand samples from natural sandy beaches will be collected. The activity concentration values of natural radionuclides ^{226}Ra , ^{232}Th and ^{40}K and anthropogenic radionuclide ^{137}Cs , as well as the radiological hazard indices associated with these activities, will be evaluated. Additionally, the results obtained will be compared with the activity concentration values of natural radionuclides from the different lithologies of the volcanic oceanic islands. This will be useful to assess the impact that the diverse geology of these islands has on the natural radioactivity levels of their beaches, as well as to evaluate the effects that anthropogenic pressure from coastal zones might have already had on them.

2. Study region

The Canary Islands are located in the North East part of the Central Atlantic Ocean (between $27^{\circ} 37' 0''$ and $29^{\circ} 25' 0''$ north latitudes and from $13^{\circ} 20' 0''$ to $18^{\circ} 10' 0''$ west longitudes), in close proximity to the Western Sahara African coast (Fig. 1). The archipelago consists of eight islands and, from an administrative perspective, they are divided into two provinces: Santa Cruz de Tenerife, comprising the four western islands (Tenerife, La Palma, La Gomera and El Hierro) and the province of Las Palmas, which covers the four eastern islands (La Graciosa, Lanzarote, Fuerteventura and Gran Canaria) and some small islets. This study is focused on the province of Las Palmas and the study region will be referred to as the Eastern Canary Islands (ECI). This is because the ECI concentrate most of the main sandy beaches of the Canary Islands and they are the 11th most populated region of Spain, with more than 1 million residents (INE, 2021a). The main industrial activity of the islands is concentrated on the island of Gran Canaria and the most developed economic sector is tourism.

From a geological point of view, these islands have a volcanic oceanic island formation. They present three different units, as described in the work by Carracedo et al. (2002). The first unit is known as the Basal Complex (or pre-shield stage), composed of turbiditic sediments intruded by sheeted dike swarms and plutonic rocks, ranging from pyroxenites to carbonatites. The second unit corresponds to the shield edifices (from basic to acid rocks) and the third unit comprises post-shield cones (rejuvenation stage with ultrabasic to acid materials). The lithology found on the different islands varies from one island to another. In La Graciosa (LG), Lanzarote (LZ) and Fuerteventura (FV) the volcanic rocks found are mostly basalts while, in Gran Canaria (GC), in addition to basalts, a considerable amount of phonolites, trachytes and rhyolites (salic materials) can be found (I.G.M.E., 2021). Previous studies of the natural radiation levels of the soils of the ECI have proved that, due to the presence of phonolites, trachytes and rhyolites in soils of GC, the natural radioactivity levels that island are above those found for LZ and FV (Arnedo et al., 2017). This is because those salic materials present naturally higher natural gamma radiation than other volcanic rocks like basalts (Chiozzi et al., 2001; Fernández-Aldecoa et al., 1992). In addition, an initial local study carried out in GC (Arnedo et al., 2013)

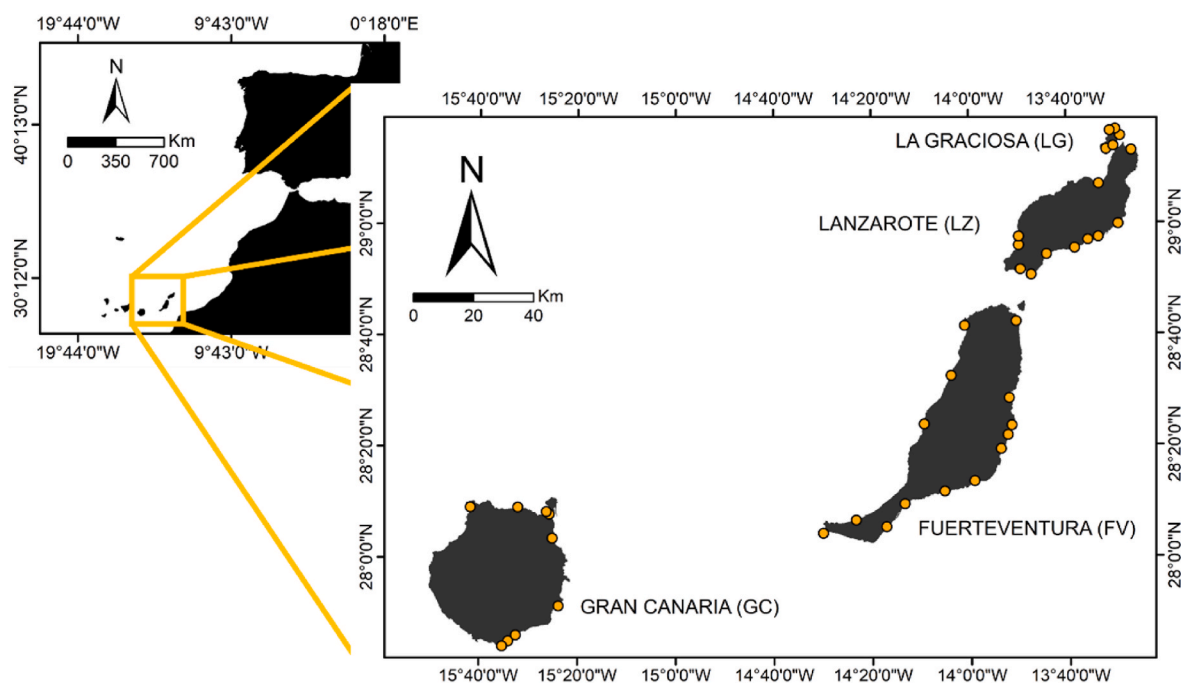


Fig. 1. Map of the location of the beach areas studied in the Eastern Canary Islands, Spain.

proved that sands from beaches that could contain salic volcanic materials (such as phonolites) presented higher activity concentration values of ^{226}Ra , ^{232}Th , and ^{40}K and higher absorbed dose rates than beaches without these materials in their sand.

3. Materials and methods

3.1. Collection and preparation of sand samples

In order to perform radiological risk assessments in beach areas, an extensive campaign was designed in the Eastern Canary Islands: i.e. La Graciosa (LG), Lanzarote (LZ), Fuerteventura (FV) and Gran Canaria (GC). A total of 108 sand samples were collected from 39 beaches spread across the four islands (Fig. 1). The coordinates of the exact sampling points on each beach are given in Table S1 (see Supplementary Appendix). Samples were collected from the intertidal zone during low tide. For each sample, a 1 m² square was drawn at each sampling point and the sand within it was mixed *in-situ*, to homogenize the sample. Then, the superficial sand sample was collected from the upper 5 cm.

After collection, all sand samples were taken to the laboratory and dried at 80 °C for 24 h. After, the samples were sieved through 1 mm mesh and stored in a PVC-trunk conical container, they were filled to 40 cm³ and sealed with aluminum strips for one month before measurement. This storage period was designed to achieve secular equilibrium between ^{226}Ra , ^{222}Rn and its short-life progenies because the gamma peak of ^{214}Pb is used to determine ^{226}Ra (Bezuidenhout, 2013).

3.2. Gamma spectrometry analysis

Radionuclides in sand samples were determined by gamma spectrometry, using a Canberra Extended Range (XtRa) Germanium (model GX3518) spectrometer, with 38% relative efficiency, with respect to a 3" x 3" active area NaI (Tl) detector, and nominal FWHM of 0.875 keV at 122 keV and 1.8 keV at 1.33 MeV. The spectrometer was coupled to a Canberra DSA-1000 multichannel analyzer with the software package Genie 2000. Efficiency calibration of the system was carried out using the Canberra LabSOCS package, based on the Monte Carlo method (Arnedo et al., 2017; Arriola-Velázquez et al., 2019, 2021; Guerra et al., 2017, 2015). For calibration, verification reference standards IAEA RGK-1 (potassium sulfate), RGU-1 (uranium ore) and RGTh-1 (thorium ore) were used. Energy calibration was performed using a $^{155}\text{Eu}/^{22}\text{Na}$ (Canberra ISOXSRCE, 7F06-9/10138 series) and confirmed using the 1460.8 keV line of ^{40}K (IAEA RGK-1) (Arnedo et al., 2017).

The radionuclides of interest were analyzed using different photopeaks. Secular equilibrium between ^{214}Bi (609.3 keV) and ^{214}Pb (351.9 keV) was confirmed experimentally and thus, to avoid the coincidence summing effect affecting ^{214}Bi photopeak, the emission line of ^{214}Pb at 351.9 keV was chosen to determine ^{226}Ra activity concentration. Additionally, it is known that the 911.6 keV photopeak of ^{228}Ac shows high uncertainties in samples with low activity concentration values of ^{232}Th . In consequence, the emission line of ^{212}Pb at 238.6 keV was selected for determining the activity concentration of ^{232}Th after verifying its equilibrium with ^{228}Ac and ^{208}Tl (583.2 keV). This is because ^{212}Pb photopeak exhibits higher intensity than ^{208}Tl and it does not present coincidence summing effect. Activity concentrations of ^{40}K and ^{137}Cs were measured directly from their emission lines at 1460.8 keV and 661.8 keV, respectively. The counting time for each sample was approximately 24 h. The activity concentration values have been expressed according to the common standard of using only one significant figure for uncertainties; a coverage factor $k = 1$ was assumed.

3.3. Statistical analysis

Once the different radiological hazard indices were obtained, a Shapiro-Wilk normality test (Shapiro and Wilk, 1965) was used to evaluate the distribution of the results. Subsequently, a Kruskal-Wallis

test (Theodorsson-Norheim, 1986) was used to evaluate the presence of significant differences in the radiological hazard indices obtained for the different islands. Moreover, a Wilcoxon rank sum test (Rosner and Glynn, 2009) was applied to identify which islands presented such differences among them. These tests were carried out with a significance level of 0.05.

4. Results and discussion

4.1. Activity concentration of ^{226}Ra , ^{232}Th and ^{40}K in the samples

The activity concentration of primordial radionuclides ^{226}Ra , ^{232}Th and ^{40}K was measured in 108 sand samples collected from 39 beaches spread across the Eastern Canary Islands: La Graciosa (LG), Lanzarote (LZ), Fuerteventura (FV) and Gran Canaria (GC). The mean activity concentration values obtained for ^{226}Ra , ^{232}Th and ^{40}K in LG were 10.9 ± 0.9 , 3.5 ± 0.4 and 49 ± 5 Bq kg⁻¹, respectively. In the case of LZ, the mean activity concentration value for ^{226}Ra was 13.3 ± 1.0 Bq kg⁻¹, for ^{232}Th a mean activity of 9.2 ± 0.6 Bq kg⁻¹ was found and for ^{40}K a mean activity concentration value of 76 ± 7 Bq kg⁻¹ was reported. In the case of FV the mean activity concentration values found for these radionuclides were 7.5 ± 0.8 Bq kg⁻¹ for ^{226}Ra , 5.6 ± 0.5 Bq kg⁻¹ for ^{232}Th and 75 ± 7 Bq kg⁻¹ for ^{40}K . Finally, for GC, the activity concentration values found for ^{226}Ra , ^{232}Th and ^{40}K were 19 ± 1 Bq kg⁻¹, 28 ± 1 Bq kg⁻¹ and 530 ± 20 Bq kg⁻¹, respectively. The results showed that, in general, all islands have activity concentration values below the world average, set at 32 Bq kg⁻¹ for ^{226}Ra , 45 Bq kg⁻¹ for ^{232}Th and 420 Bq kg⁻¹ for ^{40}K (UNSCEAR, 2000). An exception to this was found in GC, where the mean activity concentration value of ^{40}K was above the world average value. The whole list of activity concentration values obtained for each sampling point on each of the beaches studied is presented in Table S2 in the supplementary material. The relations between activity concentration of primordial radionuclides ^{226}Ra , ^{232}Th and ^{40}K in each sample are shown in Fig. 2. Additionally, the ratios of these primordial radionuclides which were found in phonolites, basalts, rhyolites and trachytes (the typical volcanic rocks that can be found in the Eastern Canary Islands), correspond to the slope of the represented color dash lines. The data from Alonso (2015) were used to calculate the ratios in the different volcanic rocks.

When observing the ratio value of $^{40}\text{K}/^{226}\text{Ra}$ (Figs. 2a) and $^{40}\text{K}/^{232}\text{Th}$ (Fig. 2b) for the volcanic rock in the Eastern Canary Islands, it would be appreciated that all of them presented higher values of ^{40}K than ^{226}Ra and ^{232}Th ; this is particularly noticeable in the phonolites. Previous studies on the Island of Tenerife and in the Aeolian volcanic arc in Italy (both volcanic settlements) showed that phonolites, along with trachytes and rhyolites, are the rocks that present higher natural gamma radiation (Chiozzi et al., 2001; Fernández-Aldecoa et al., 1992). According to the Total Alkalinity Silica (TAS) diagram (Le Bas et al., 1986), phonolites are in the group of volcanic rocks that have the highest content of potassium (see Fig. S1). Therefore, these types of volcanic rocks would naturally have a higher ^{40}K content and this explains why they have higher activity concentration values of this gamma emitter). In the case of the $^{226}\text{Ra}/^{232}\text{Th}$ ratio (Fig. 2c), the phonolites and trachytes present a higher ^{232}Th content than ^{226}Ra . This contrasts with basalts, where these radionuclides seem to be in equilibrium, and rhyolites, that present slightly higher activity concentration values of ^{226}Ra .

Regarding the $^{40}\text{K}/^{226}\text{Ra}$ (Figs. 2a) and $^{40}\text{K}/^{232}\text{Th}$ (Fig. 2b) ratios in samples from La Graciosa, Lanzarote, Fuerteventura and Gran Canaria, it can be appreciated that the samples from the beaches of GC generally presented ratios (proportion of ^{40}K to ^{226}Ra and proportion of ^{40}K to ^{232}Th) higher than those found on the other islands, being even higher than the typical value found for phonolites in the ECI. In addition, the $^{226}\text{Ra}/^{232}\text{Th}$ ratio (Fig. 2c) showed that in general the samples from the beaches of GC presented lower ratios than the samples from the beaches of LG, LZ and FV. These results show that the samples from GC followed a similar pattern in their ratios to the phonolites and trachytes.

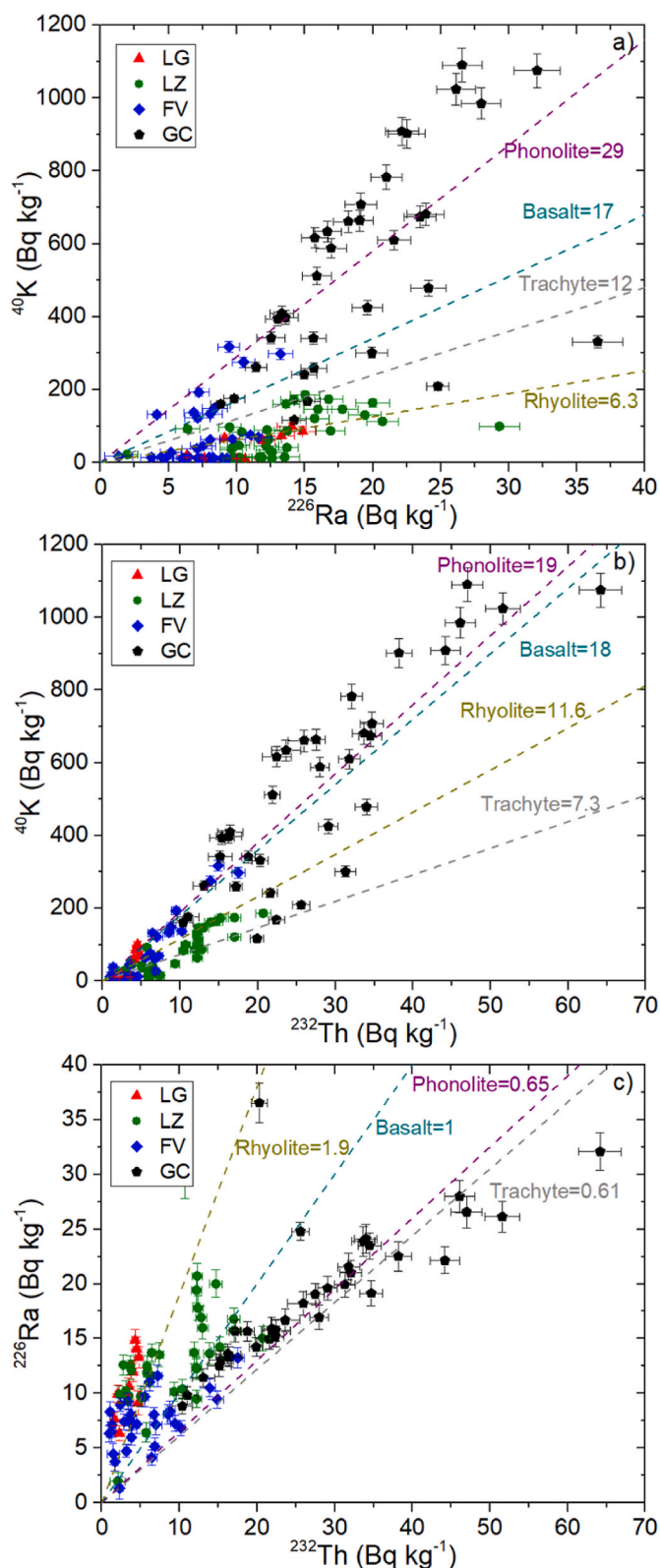


Fig. 2. Activity concentration values of a) ^{40}K vs ^{226}Ra , b) ^{40}K vs ^{232}Th and c) ^{226}Ra vs ^{232}Th obtained for all sand samples in the different islands. Slopes of dash lines are the ratios calculated for different volcanic rocks from the data of Alonso (2015).

In the work of Arnedo et al. (2017), the activity concentration values of ^{226}Ra , ^{232}Th and ^{40}K were mapped in the soils of the Eastern Canary Islands. The results showed that, on GC, the maximum activity concentration values of ^{226}Ra ($>50 \text{ Bq kg}^{-1}$), ^{232}Th ($>90 \text{ Bq kg}^{-1}$) and ^{40}K ($>1000 \text{ Bq kg}^{-1}$) were considerably higher than FV and LZ. This was related to the fact that in GC some volcanic rocks with high activity concentration values of ^{226}Ra , ^{232}Th and ^{40}K (such as phonolites and trachytes) could be found. In the other islands studied in that work, the geological composition of the soils was mostly basalts, which explained the lower activity concentration values found there in comparison to GC. In this study, the activity concentration values found in the beaches from GC are also higher than in the beaches from FV, LZ and LG. This is because the sediments that compose the beach sands of each island have its terrigenous source in the different rocks that can be found in them. Thus, differences in the activity concentration values found in sand samples from GC and the other islands seem to reflect the geological variations in the terrigenous source of sediments that can be found in the different islands.

4.2. Radiological risk assessment

4.2.1. The absorbed dose rate (nGy h^{-1}) and annual effective dose rate (mSv y^{-1})

The absorbed dose rate (D), in nGy h^{-1} , due to natural radio-isotopes at a height of 1 m above ground level, was calculated by using equation (1) (UNSCEAR, 2008, 2000):

$$D = 0.462A_{\text{Ra}} + 0.0417A_{\text{K}} + 0.604A_{\text{Th}} \quad (1)$$

where A_{Ra} , A_{K} and A_{Th} are the respective activity concentrations of ^{226}Ra , ^{40}K and ^{232}Th in Bq kg^{-1} . The mean dose rate obtained for each of the beaches studied is given in Table 1. For the ECI, the absorbed dose rate ranged from 3.1 to 72.6 nGy h^{-1} , with an average value of 20.8 nGy h^{-1} . The mean value obtained in this study was below the Spanish mean of 76 nGy h^{-1} and below the world average of 57 nGy h^{-1} (UNSCEAR, 2000). Nevertheless, at some locations on GC (e.g. El Inglés Beach and Maspalomas Beach), the values obtained were above the world average. Despite this, the mean absorbed dose rate obtained for the ECI was similar to others obtained from different parts of the Atlantic coast. A mean value of 20.6 nGy h^{-1} was found in Venezuela (Alfonso et al., 2014) and an average value of 26.8 nGy h^{-1} in the coast of Senegal (Dione et al., 2018). However, the mean value obtained for the absorbed dose rate in this study was relatively low, in comparison with other parts of the world, such as the coast of the Red Sea in Egypt, where a mean value of 38 nGy h^{-1} was found (Zakaly et al., 2021) or the east coast of Tamilnadu in India, where a value of 86.9 nGy h^{-1} was reported (Ravisankar et al., 2015). Additionally, much higher values have been found in other parts of the world, e.g. in Bahia (Brazil), where a value of 1792 nGy h^{-1} was reported (Vasconcelos et al., 2011), parts of Malaysia, where a value of 1748 nGy h^{-1} was found (Shuaibu et al., 2017) or in Mandaikadu in India where an absorbed dose rate of 4722 nGy h^{-1} was reported (Thangam et al., 2022). In all these cases, the high absorbed dose rate was related to the presence of monazite in the samples. This shows that the geological nature of the sediments found on beaches seems to influence the radiological risk caused by them.

Due to the warm weather that the ECI have all year long, the residents of the islands and the long-time visitors spend time on the beaches all year long as well as there are beach workers that everyday spend hours on them. Thus, the outdoor annual effective dose (AEDE), another type of absorbed dose in mSv y^{-1} , was calculated according to (UNSCEAR, 2008, 2000):

$$\text{AEDE} = D \times F \times T \times O \times 10^{-6} \quad (2)$$

where D is the external dose rate (given in nGy h^{-1}), F is the absorbed dose to effective dose conversion factor (0.7 Sv Gy^{-1}), T is hours per year (8760 h y^{-1}), O is the occupancy factor (0.2) and 10^{-6} is the nano to

Table 1

Mean Absorbed dose rate (D) in nGy h⁻¹, Annual effective dose (AEDE) in mSv y⁻¹, Excess life cancer risk (ELCR) and Radium equivalent (Ra_{eq}) in Bq kg⁻¹ obtained for each beach studied.

Island	Beach	D	AEDE	ELCR (× 10 ⁻³)	Ra _{eq}
LG	Pedro Barbas	7.5	0.009	0.04	16.46
LG	Playa del Ambar	6.3	0.008	0.03	13.68
LG	Las Conchas	5.1	0.006	0.03	11.02
LG	Francesa	10.8	0.013	0.06	23.07
LG	Caleta Sebo	13.2	0.016	0.07	27.89
Mean value in LG		8.6	0.010	0.05	18.42
LZ	Orzola	3.1	0.004	0.02	6.63
LZ	Teguise	12.4	0.015	0.07	27.24
LZ	Arrecife	9.7	0.012	0.05	21.08
LZ	Honda	22.6	0.028	0.12	48.63
LZ	Pto. Carmen	19.8	0.024	0.11	43.01
LZ	Quemada	27.2	0.033	0.15	58.96
LZ	Papagayo	7.2	0.009	0.04	15.84
LZ	P.BlancaLZ	9.6	0.012	0.05	20.53
LZ	Janubio	25.1	0.031	0.14	54.17
LZ	Hervideros	22.8	0.028	0.13	49.04
LZ	Famara	12.6	0.015	0.07	27.71
Mean value in LZ		15.6	0.019	0.09	33.89
FV	Corralejo	5.1	0.006	0.03	10.97
FV	P. BlancaFV	13.5	0.017	0.07	28.51
FV	Caleta de Fuste	10.5	0.013	0.06	22.54
FV	Salinas del Carmen	12.6	0.015	0.07	27.26
FV	Pozo Negro	15.4	0.019	0.09	32.45
FV	Las Playitas	11.3	0.014	0.06	23.52
FV	Gran Tarajal	23.6	0.029	0.13	49.46
FV	Costa Calma	8.7	0.011	0.05	18.97
FV	Jandia	7.1	0.009	0.04	15.51
FV	La Punta	7.7	0.009	0.04	17.09
FV	Cofete	7.5	0.009	0.04	16.08
FV	Ajuy	15	0.018	0.08	31.98
FV	Los Molinos	26.6	0.033	0.15	55.16
FV	El Cotillo	4.3	0.005	0.02	9.57
Mean value in FV		12.1	0.015	0.07	25.65
GC	El Puertito de Bañaderos	44.4	0.054	0.25	93.95
GC	Sardina del Norte	35.6	0.044	0.20	77.5
GC	La Laja	35.8	0.044	0.20	77.34
GC	Arinaga	33.8	0.041	0.19	71.92
GC	El Inglés	72.6	0.089	0.40	151.06
GC	Las Alcaravaneras	45.6	0.056	0.25	94.45
GC	Maspalomas	67.5	0.083	0.37	139.63
GC	San Agustín	57.9	0.071	0.32	120.6
GC	Las Canteras	33.3	0.041	0.18	68.78
Mean value in GC		47.4	0.058	0.26	99.47
Total mean value		20.8	0.025	0.11	44.08

milli conversion factor. The results obtained for the ECI show an average value of 0.025 mSv y⁻¹, which is below the world mean value of 0.07 mSv y⁻¹ (UNSCEAR, 2000). However, in the case of El Inglés Beach, Maspalomas and San Agustín (all located in GC), the values obtained (Table 1) are higher than the world average. Nevertheless, all the values obtained in this study were below the maximum of 1 mSv y⁻¹ recommended for the general public (ICRP, 2007). Considering the results obtained for the absorbed dose rate and the annual effective dose, the studied area does not pose a considerable radiological threat to the public. Moreover, it is noteworthy that in this radiological analysis, no ¹³⁷Cs was detected above the minimum detectable activity (MDA) that for our samples ranged between 2 and 3 Bq kg⁻¹.

4.2.2. Excess life cancer risk

The Excess life cancer risk (ELCR) gives information about the risk of developing cancer over a lifetime due to an exposure at a given radiation level. It is calculated using equation (3) (Al Shaaibi et al., 2023; Kolo et al., 2015):

$$ELCR = AEDE \times DL \times RF \quad (3)$$

where AEDE is the annual effective dose, in mSv y⁻¹, DL is the life expectancy (established as 82 for the Eastern Canary Islands, according to

the Spanish National Statistics Institute (INE, 2021b)) and RF is the detriment-adjusted nominal risk coefficient for cancer, set at 0.055 Sv⁻¹ (ICRP, 2007). The results for the ECI given in Table 1 ranged from 0.02–0.40 × 10⁻³ with a mean value of 0.11 × 10⁻³. The world average for the ELCR is set at 0.29 × 10⁻³ (Abdullahi et al., 2019; Al Shaaibi et al., 2023; Mohammed and Ahmed, 2017). This means that, even though the ELCR coefficient is higher than the world average (Table 1) on some beaches from GC (El Inglés Beach, Maspalomas and San Agustín), the ELCR is below the world average value on most of the beaches of the Eastern Canary Islands.

4.2.3. Radium equivalent

The Radium equivalent activity (Ra_{eq}) calculation assumes that the gamma dose rate produced by 370 Bq kg⁻¹ of ²²⁶Ra, 259 Bq kg⁻¹ of ²³²Th or 4810 Bq kg⁻¹ of ⁴⁰K is the same (Beretka and Mathew, 1985). Therefore, it allows the comparison of the radiological risks of different samples combining the activity concentration values of ²²⁶Ra, ²³²Th and ⁴⁰K it is calculated from equation (4) (Beretka and Mathew, 1985; Elisha et al., 2013):

$$Ra_{eq} = A_{Ra} + 1.43A_{Th} + 0.077A_K \quad (4)$$

where A_{Ra}, A_K and A_{Th} are the respective activity concentrations of ²²⁶Ra, ⁴⁰K and ²³²Th in Bq kg⁻¹. In the case of the beaches on the Eastern Canary Islands, the values of the Ra_{eq} ranged between 6.63 and 151.06 Bq kg⁻¹ with a mean value of 44.08 Bq kg⁻¹. These values are comparable with values found in other parts of the world, such as the Mediterranean coast from Egypt where Ra_{eq} ranged between 38.7 and 116.3 Bq kg⁻¹ in beach sand samples with a mean value of 61.1 Bq kg⁻¹ (Awad et al., 2022). Additionally, some of the results obtained in this work for Ra_{eq} are two or three times higher than other values that can be found around the world, like in the work of (Khandaker et al., 2019) where Ra_{eq} ranged between 37 and 50 Bq kg⁻¹ and a mean value of 45.4 Bq kg⁻¹ was reported. However, all values obtained in this world are below the safe limit of 370 Bq kg⁻¹ (Beretka and Mathew, 1985).

4.3. Differences in the radiological hazard indices between the different Eastern Canary Islands

As mentioned in Subsection 4.2 (Radiological risk assessment), the radiological risk indices ranged widely between the beaches studied, with some of them having very low values and others having values higher than the world average. In fact, when comparing the mean hazard indices obtained for each island (Table 1), it can be seen that the mean values on the island of GC are considerably higher than the other islands, sometimes up to more than four times higher. In order to evaluate whether the differences found between the islands were significant, a Kruskal-Wallis test (Theodorsson-Norheim, 1986) and a Wilcoxon-rank sum test (Rosner and Glynn, 2009) were used. The results of these tests are represented in Table 2 and it can be seen that all of the radiological hazard index values obtained in GC were significantly different from the values obtained on the other islands. In addition, the values from LZ also showed significant differences from the values obtained from FV.

Fig. 3 shows the mean absorbed dose rate for each of the beaches studied, along with the geological map of the Eastern Canary Islands. The lithology on the geological map is represented following the same classification that Briones et al. (2023) obtained from the lithostratigraphic map of the Canary Islands, produced by the Spanish Geological and Mining Institute (I.G.M.E., 2021). According to this classification, the term 'Acidic' refers to intermediate and acid rocks such as phonolites, trachytes, trachybasalts, rhyolites, and syenites (and deposits formed from these rocks). The 'Basic' group includes basalts, basanites, tephrites, and phonolitic tephrites (and deposits formed from these rocks). 'Clays' include lake soils and sandy-clay soils. The term 'Deposits' refers to sand deposits and debris of generally variable

Table 2

Result of the Kruskal-Wallis test for identifying significant differences in the radiological hazard indices and the activity concentration values of ²²⁶Ra, ²³²Th and ⁴⁰K obtained for each sample and grouped by the island where they are located. The result of the p-value for the Wilcoxon rank sum test is also displayed in brackets to identify the groups that present significant differences between them.

Radiological hazard indices	Kruskal-Wallis p-value	Wilcoxon rank sum test
Absorbed dose rate (D)	5.1×10^{-15}	LZ-FV (5.0×10^{-3}) GC-LG (1.4×10^{-8}) GC-LZ (1.9×10^{-14}) GC-FV (2.4×10^{-15})
Annual effective doce (AEDE)	5.1×10^{-15}	LZ-FV (5.0×10^{-3}) GC-LG (1.4×10^{-8}) GC-LZ (1.9×10^{-14}) GC-FV (2.4×10^{-15})
Excess life cancer risk (ELCR)	5.1×10^{-15}	LZ-FV (5.0×10^{-3}) GC-LG (1.4×10^{-8}) GC-LZ (1.9×10^{-14}) GC-FV (2.4×10^{-15})
Radium equivalent (Ra _{eq})	4.4×10^{-15}	LZ-FV (4.3×10^{-3}) GC-LG (1.4×10^{-8}) GC-LZ (2.3×10^{-14}) GC-FV (1.8×10^{-15})
²²⁶ Ra	7.7×10^{-14}	LZ-FV (4.1×10^{-9}) GC-LG (1.3×10^{-4}) GC-LZ (1.1×10^{-4}) GC-FV (3.2×10^{-15})
²³² Th	7.1×10^{-15}	LZ-FV (1.1×10^{-2}) GC-LG (1.4×10^{-8}) GC-LZ (7.3×10^{-10}) GC-FV (1.8×10^{-15})
⁴⁰ K	4.9×10^{-14}	GC-LG (2.1×10^{-5}) GC-LZ (2.8×10^{-11}) GC-FV (2.3×10^{-13})

Kruskal-Wallis p-value 0.05.
Wilcoxon rank sum test 0.05.

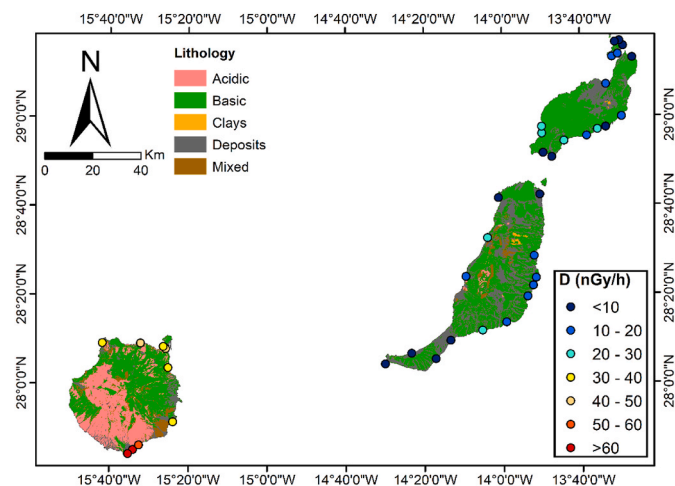


Fig. 3. Map of the mean absorbed dose rate (D) in nGy h⁻¹ in each beach area studied combined with the geological map of the Eastern Canary Islands.

composition, depending on the surrounding lithology. Finally, the group labelled ‘Mixed’ includes lithology that combines volcanic rocks from the Acidic and Basic groups without the possibility of differentiating them.

When comparing the doses obtained for each island, by the different lithologies, it can be seen that the doses on GC are higher than for the rest of the islands. Regarding the lithology, GC also presents the highest content of acidic rocks, while LG, LZ and FV have a mostly basic lithology. As mentioned in Subsection 4.1 (Activity concentration of ²²⁶Ra, ²³²Th and ⁴⁰K in the samples), the acidic lithology was found to have

higher contents of ²²⁶Ra, ²³²Th and ⁴⁰K. Hence, the external hazard indices, which are calculated from the activity concentration values of ²²⁶Ra, ²³²Th and ⁴⁰K, would be higher in these types of volcanic rocks. It can be seen that, in the southern parts of GC, where most of the acidic rocks are located, the highest absorbed dose rates can be found, these values being above the world mean value of 57 nGy h⁻¹ (UNSCEAR, 2000). This suggests that, for the beaches of the Eastern Canary Islands, the radiological hazard indices highly depend on the lithology of the sediments that comprise the sand. This is similar to some of the beaches in Brazil and Malaysia (Shuaibu et al., 2017; Vasconcelos et al., 2011), where the presence of monazite caused high activity concentration values of ²³²Th and, thus, the absorbed dose rates were higher than the world average.

In the case of LZ and FV, even though some significant differences were found for these islands when observing the map in Fig. 3, the absorbed dose rate differences were not as strong as those found for GC and the other islands. This is because the types of rocks that can be found in Lanzarote and Fuerteventura are similar and thus these significant differences could not be explained in relation to the changes in geology between the islands. To better understand why these differences appeared, a Kruskal-Wallis and a Wilcoxon-rank sum test were also performed to the activity concentration values of ⁴⁰K, ²²⁶Ra and ²³²Th found in each island (Table 2) to assess which radionuclide was responsible for the significant differences in the radiological hazard indices between FV and LZ. The results show that these two islands presented significant differences only in the activity concentration values of ²²⁶Ra and ²³²Th with a p-value from the Wilcoxon-rank sum test of 4.1×10^{-9} and 1.1×10^{-2} respectively. Considering that the highest activity concentration value of ²²⁶Ra was found in Playa Honda (29 ± 1 Bq kg⁻¹) and the maximum activity concentration of ²³²Th (20.7 ± 1.0 Bq kg⁻¹) was found in Playa Quemada (both beaches located in the most populated coast of LZ), it seems that the differences in absorbed dose rate between LZ and FV could be related to some anthropogenic influences. However, further studies are necessary to better understand the significant differences between these two islands.

5. Conclusions

A baseline of the environmental background radioactivity has been established for beaches of the Eastern Canary Island. The activity concentration values of natural radionuclides ²²⁶Ra, ²³²Th and ⁴⁰K in intertidal sand samples were analyzed and the radiological hazard indices associated to them were calculated. The mean absorbed dose rate had a value of 20.8 nGy h⁻¹, the mean annual effective dose was 0.025 mSv y⁻¹, the mean Excess life cancer risk value was of 0.11×10^{-3} and the mean radium equivalent obtained was 44.08 Bq kg⁻¹. All these values were below the international accepted limit for each radiological hazard index. Moreover, no ¹³⁷Cs was detected above the MDA. Thus, the beaches of the Eastern Canary Island do not pose a radiological risk for the public. Additionally, the activity concentration values of ²²⁶Ra, ²³²Th and ⁴⁰K, as well as the radiological hazard indices associated to them, were significantly higher in Gran Canaria than in the other islands. This seems to be due to the presence of lithologies with high activity concentrations of natural radionuclides, such as phonolites or trachytes, in Gran Canaria. In the case of Lanzarote and Fuerteventura, significant differences were also found between the islands, with Lanzarote presenting significantly higher radiological hazard indices and activity concentration values of ²²⁶Ra and ²³²Th. The lithologies in Lanzarote and Fuerteventura are similar and, considering that the highest activity concentration values of ²²⁶Ra and ²³²Th are present in the most urbanized coast of Lanzarote, it seems that these differences could be related to the anthropogenic pressure that the coast of Lanzarote has already suffered. Finally, this study establishes a methodology to determine the baseline levels of environmental background radioactivity in sandy beaches from volcanic oceanic islands. In addition, it provides a useful tool for authorities to detect future radiological

impacts on the coastal areas of the islands.

Author contributions statement

Ana del Carmen Arriola-Velázquez: methodology, formal analysis, investigation, writing - original draft, visualization. **Alicia Tejera:** methodology, investigation, supervision. **Héctor Alonso:** investigation. **Neus Miquel-Armengol:** data curation. **Jesús G. Rubiano:** conceptualization, supervision. **Pablo Martel:** conceptualization, methodology, investigation, writing - review & editing, supervision.

Declaration of competing interest

The authors declare that they have no known competing financial interests or personal relationships that could have appeared to influence the work reported in this paper.

Data availability

Data are available in the supplementary material file.

Acknowledgments

The lithostratigraphic maps were obtained from Cartografía Digital del Mapa Geológico y Continuo de España (GEODE) and were supplied by Instituto Geológico y Minero de España (I.G.M.E.).

Appendix A. Supplementary data

Supplementary data to this article can be found online at <https://doi.org/10.1016/j.envpol.2023.122809>.

References

- Abbasi, A., Zakaly, H.M.H., Mirekhtyari, F., 2020. Baseline levels of natural radionuclides concentration in sediments East coastline of North Cyprus. *Mar. Pollut. Bull.* 161, 111793. <https://doi.org/10.1016/j.marpolbul.2020.111793>.
- Abdullahi, S., Ismail, A.F., Samat, S., 2019. Determination of indoor doses and excess lifetime cancer risks caused by building materials containing natural radionuclides in Malaysia. *Nucl. Eng. Technol.* 51, 325–336. <https://doi.org/10.1016/j.net.2018.09.017>.
- Akpan, A.E., Ebong, E.D., Ekwok, S.E., Eyo, J.O., 2020. Assessment of radionuclide distribution and associated radiological hazards for soils and beach sediments of Akwa Ibom Coastline, southern Nigeria. *Arabian J. Geosci.* 13, 753. <https://doi.org/10.1007/s12517-020-05727-7>.
- Al Shaaibi, M., Ali, J., Tsikouras, B., Masri, Z., 2023. Environmental radioactivity assessment of the Brunei Darussalam coastline of the South China Sea. *Environ. Pollut.* 323, 121288. <https://doi.org/10.1016/j.envpol.2023.121288>.
- Alfonso, J.A., Pérez, K., Palacios, D., Handt, H., LaBrecque, J.J., Mora, A., Vásquez, Y., 2014. Distribution and environmental impact of radionuclides in marine sediments along the Venezuelan coast. *J. Radioanal. Nucl. Chem.* 300, 219–224. <https://doi.org/10.1007/s10967-014-2999-z>.
- Alonso, H., 2015. El radón en suelos, rocas, materiales de construcción y aguas subterráneas de las Islas Canarias Orientales. Universidad de Las Palmas de Gran Canaria, Las Palmas de Gran Canaria.
- Alonso, H., Cruz-Fuentes, T., Rubiano, J.G., González-Guerra, J., Cabrera, M., del, C., Arnedo, M.A., Tejera, A., Rodríguez-Gonzalez, A., Pérez-Torrado, F.J., Martel, P., 2015. Radon in groundwater of the northeastern gran Canaria aquifer. *Water (Basel)* 7, 2575–2590. <https://doi.org/10.3390/w7062575>.
- Arnedo, M.A., Tejera, A., Rubiano, J.G., Alonso, H., Gil, J.M., Rodríguez, R., Martel, P., 2013. Natural radioactivity measurements of beach sands in gran Canaria, Canary Islands (Spain). *Radiat. Protect. Dosim.* 156, 75–86. <https://doi.org/10.1093/rpd/ncd044>.
- Arnedo, M.A., Rubiano, J.G., Alonso, H., Tejera, A., González, A., González, J., Gil, J.M., Rodríguez, R., Martel, P., Bolívar, J.P., 2017. Mapping natural radioactivity of soils in the eastern Canary Islands. *J. Environ. Radioact.* 166, 242–258. <https://doi.org/10.1016/j.jenvrad.2016.07.010>.
- Arriola-Velázquez, A., Tejera, A., Guerra, J.G., Alonso, I., Alonso, H., Arnedo, M.A., Rubiano, J.G., Martel, P., 2019. Spatio-temporal variability of natural radioactivity as tracer of beach sedimentary dynamics. *Estuar. Coast Shelf Sci.* 231. <https://doi.org/10.1016/j.ecss.2019.106476>.
- Arriola-Velázquez, A.C., Tejera, A., Guerra, J.G., Geibert, W., Stimac, I., Cámara, F., Alonso, H., Rubiano, J.G., Martel, P., 2021. ^{226}Ra , ^{228}Ra and ^{40}K as tracers of erosion and accumulation processes: a 3-year study on a beach with different sediment dynamics. *Catena* 207, 105705. <https://doi.org/10.1016/j.catena.2021.105705>.
- I.G.M.E., 2021. Cartografía digital del Mapa Geológico y Continuo de España GEODE (Comunidad autónoma de Canarias). Instituto Geológico y Minero de España.
- Awad, M., El Mezayen, A.M., El Azab, A., Alfi, S.M., Ali, H.H., Hanfi, M.Y., 2022. Radioactive risk assessment of beach sand along the coastline of Mediterranean Sea at El-Arish area, North Sinai, Egypt. *Mar. Pollut. Bull.* 177, 113494. <https://doi.org/10.1016/j.marpolbul.2022.113494>.
- Beretka, J., Mathew, P.J., 1985. Natural radioactivity of Australian building materials, industrial wastes and by-products. *Health Phys.* 48, 87–95.
- Bezuidenhout, J., 2013. Measuring naturally occurring uranium in soil and minerals by analysing the 352keV gamma-ray peak of ^{214}Pb using a NaI(Tl)-detector. *Appl. Radiat. Isot.* 80, 1–6. <https://doi.org/10.1016/j.apradiso.2013.05.008>.
- Bou-Rabee, F., Al-Zamel, A., Al-Fares, R., Bem, H., 2009. Technologically enhanced naturally occurring radioactive materials in the oil industry (TENORM). A review. *NUKLEONIKA* 54, 3–9.
- Briones, C., Jubera, J., Alonso, H., Olaiz, J., Santana, J.T., Rodríguez-Brito, N., Arriola-Velázquez, A.C., Miquel, N., Tejera, A., Martel, P., González-Díaz, E., Rubiano, J.G., 2023. Multiparametric analysis for the determination of radon potential areas in buildings on different soils of volcanic origin. *Sci. Total Environ.* 885, 163761. <https://doi.org/10.1016/j.scitotenv.2023.163761>.
- Carracedo, J.C., Pérez-Torrado, F.J., Ancochea, E., Meco, J., Hernán, F., Cubas, C.R., Casillas, R., Rodríguez Badiola, E., Ahijado, A., 2002. Cenozoic Volcanism II: Canary Islands. Geological Society.
- Chiozzi, P., Pasquale, V., Verdoya, M., Minato, S., 2001. Natural gamma-radiation in the Aeolian volcanic arc. *Appl. Radiat. Isot.* 55, 737–744.
- Elisha, J.J., Yisa, J., Adeyemo, D.J., 2013. Radiological analysis of selected organic fertilizers in zaria local government area council, kaduna state, Nigeria: possible health implications. *IOSR J. Appl. Phys.* 5, 44–48.
- Fernández-Aldecoa, J.C., Robayna, B., Allende, A., Poffijn, A., Hernández-Armas, J., 1992. Natural radiation in Tenerife (canary islands). *Radiat. Protect. Dosim.* 45, 545–548.
- Froehlich, K., 2010. Environmental Radionuclides: Tracers and Timers of Terrestrial Processes, First. ed. Elsevier B.V., Amsterdam. [https://doi.org/10.1016/S1569-4860\(09\)01613-1](https://doi.org/10.1016/S1569-4860(09)01613-1).
- Guerra, J.G., Rubiano, J.G., Winter, G., Guerra, A.G., Alonso, H., Arnedo, M.A., Tejera, A., Gil, J.M., Rodríguez, R., Martel, P., Bolívar, J.P., 2015. A simple methodology for characterization of germanium coaxial detectors by using Monte Carlo simulation and evolutionary algorithms. *J. Environ. Radioact.* 149, 8–18. <https://doi.org/10.1016/j.jenvrad.2015.06.017>.
- Guerra, J.G., Rubiano, J.G., Winter, G., Guerra, G., A, Alonso, H., Arnedo, M.A., Tejera, A., Martel, P., Bolívar, J.P., 2017. Computational characterization of HPGe detectors useable for a wide variety of source geometries by using Monte Carlo simulation and a multi-objective evolutionary algorithm. *Nucl. Instrum. Methods Phys. Res.* 858, 113–122. <https://doi.org/10.1016/j.nima.2017.02.087>.
- ICRP, 2007. The 2007 Recommendations of the International Commission on Radiological Protection. ELSEVIER.
- INE, 2021a. Instituto Nacional de Estadística [WWW Document]. Cifras oficiales de población resultantes de la revisión del Padrón municipal a 1 de enero. URL <https://www.ine.es/jaxiT3/Datos.htm?t=2852#?tabs=tabla> (accessed July.16.2023).
- INE, 2021b. Instituto Nacional de Estadística [WWW Document]. Indicadores de Mortalidad. URL <https://www.ine.es/jaxiT3/Datos.htm?t=1485> (accessed July.14.2023).
- INE, 2022. Instituto Nacional de Estadística [WWW Document]. Movimientos Turísticos en Fronteras. URL <https://www.ine.es/jaxiT3/Datos.htm?t=23988> (accessed July.16.2023).
- Jaffary, Md, N, A., Khoo, K.S., Mohamed, N.H., Yusof, M.A.W., Mohd Fadzil, S., 2019. Malaysian monazite and its processing residue: chemical composition and radioactivity. *J. Radioanal. Nucl. Chem.* 322, 1097–1105. <https://doi.org/10.1007/s10967-019-06813-1>.
- Khandaker, M.U., Garba, N.N., Rohaizad, C.A.H.B.C., Bradley, D.A., 2019. Assessment of natural radioactivity levels in stony sand from black stone beach of kuantan, the peninsular Malaysia. *Radioprotection* 54, 211–218. <https://doi.org/10.1051/radiopro/2019024>.
- Kolo, M.T., Aziz, S.A.B.A., Khandaker, M.U., Asaduzzaman, K., Amin, Y.M., 2015. Evaluation of radiological risks due to natural radioactivity around Lynas Advanced Material Plant environment, Kuantan, Pahang, Malaysia. *Environ. Sci. Pollut. Control Ser.* 22, 13127–13136. <https://doi.org/10.1007/s11356-015-4577-5>.
- Le Bas, M.J., Le Maitre, R.W., Streckeisen, A., Zanettin, B., 1986. A chemical classification of volcanic rocks based on the total alkali-silica diagram. *J. Petrol.* 27, 745–750.
- Licínio, M.V., Alencar, A.S. de, Lima, A.C., de Freitas, A.C., 2021. Natural radioactivity at beach sands in ilha grande, southeastern Brazil. *J. Radioanal. Nucl. Chem.* 327, 1277–1281. <https://doi.org/10.1007/s10967-020-07587-7>.
- MarineTraffic, 2023. MarineTraffic: Global Ship Tracking Intelligence | AIS Marine Traffic [WWW Document]. URL <https://www.marinetraffic.com/en/ais/home/cent-erx-13.9/centery:28.2/zoom:8> (accessed July.16.2023).
- Mohammed, R.S., Ahmed, R.S., 2017. Estimation of excess lifetime cancer risk and radiation hazard indices in southern Iraq. *Environ. Earth Sci.* 76. <https://doi.org/10.1007/s12665-017-6616-7>.
- Rao, N.S., Sengupta, D., Guin, R., Saha, S.K., 2009. Natural radioactivity measurements in beach sand along southern coast of Orissa, Eastern India. *Environ. Earth Sci.* 59, 593–601. <https://doi.org/10.1007/s12665-009-0057-x>.
- Ravisankar, R., Chandramohan, J., Chandrasekaran, A., Prince Prakash Jebakumar, J., Vijayalakshmi, I., Vijayagopal, P., Venkatraman, B., 2015. Assessments of radioactivity concentration of natural radionuclides and radiological hazard indices in sediment samples from the East coast of Tamilnadu, India with statistical

- approach. *Mar. Pollut. Bull.* 97, 419–430. <https://doi.org/10.1016/j.marpolbul.2015.05.058>.
- Rosner, B., Glynn, R.J., 2009. Power and sample size estimation for the wilcoxon rank sum test with application to comparisons of C statistics from alternative prediction models. *Biometrics* 65, 188–197. <https://doi.org/10.1111/j.1541-0420.2008.01062.x>.
- Shapiro, S.S., Wilk, M.B., 1965. An analysis of variance test for normality (complete samples). *Biometrika* 52, 591–611. <https://doi.org/10.2307/2333709>.
- Shuaibu, H.K., Khandaker, M.U., Alrefae, T., Bradley, D.A., 2017. Assessment of natural radioactivity and gamma-ray dose in monazite rich black Sand Beach of Penang Island, Malaysia. *Mar. Pollut. Bull.* 119, 423–428. <https://doi.org/10.1016/j.marpolbul.2017.03.026>.
- Thangam, V., Rajalakshmi, A., Chandrasekaran, A., Arun, B., Viswanathan, S., Venkatraman, B., Bera, S., 2022. Determination of natural radioactivity in beach sands collected along the coastal area of Tamilnadu, India using gamma ray spectrometry. *J. Radioanal. Nucl. Chem.* 331, 1207–1223. <https://doi.org/10.1007/s10967-022-08193-5>.
- Theodorsson-Norheim, E., 1986. Kruskal-Wallis test: BASIC computer program to perform nonparametric one-way analysis of variance and multiple comparisons on ranks of several independent samples. *Comput. Methods Progr. Biomed.* 23, 57–62. [https://doi.org/10.1016/0169-2607\(86\)90081-7](https://doi.org/10.1016/0169-2607(86)90081-7).
- Tichavska, M., Tovar, B., 2015. Environmental cost and eco-efficiency from vessel emissions in Las Palmas Port. *Transp Res E Logist Transp Rev* 83, 126–140. <https://doi.org/10.1016/j.tre.2015.09.002>.
- UNSCEAR, 2000. Sources and effects of ionizing radiation. Report of the United Nations Scientific Committee on the Effects of Atomic Radiation to the General Assembly, with Scientific Annexes. United Nations, New York.
- UNSCEAR, 2008. Sources and effects of ionizing radiation. Report of the United Nations Scientific Committee on the Effects of Atomic Radiation to the General Assembly, with Scientific Annexes. United Nations, New York.
- Vasconcelos, D.C., Pereira, C., Oliveira, A.H., Santos, T.O., Rocha, Z., de, B.C., Menezes, M.Á., 2011. Determination of natural radioactivity in beach sand in the extreme south of Bahia, Brazil, using gamma spectrometry. *Radiat. Protect. Environ.* 34, 178–184.
- Vineethkumar, V., Akhil, R., Shimod, K.P., Prakash, V., 2020. Geospatial analysis of the source of monazite deposits and the dynamics of natural radionuclides in the selected coastal environs of Kerala, south west coast of India. *J. Radioanal. Nucl. Chem.* 326, 983–996. <https://doi.org/10.1007/s10967-020-07418-9>.
- Zakaly, H.M.H., Uosif, M.A.M., Issa, S.A.M., Tekin, H.O., Madkour, H., Tammam, M., El-Taher, A., Alharshan, G.A., Mostafa, M.Y.A., 2021. An extended assessment of natural radioactivity in the sediments of the mid-region of the Egyptian Red Sea coast. *Mar. Pollut. Bull.* 171, 112658 <https://doi.org/10.1016/j.marpolbul.2021.112658>.